The potential of graphene as an ITO replacement in organic solar cells: An optical perspective

Wee Shing Koh, *Member, IEEE,* Choon How Gan, Wee Kee Phua, Yuriy A. Akimov and Ping Bai *Member, IEEE*

***Abstract*—Graphene possesses innate potential to replace ITO as the transparent electrode in an organic solar cell device. From our transmittance study weighted with the Air Mass 1.5 Global solar spectrum, it is found that a higher transparency may be obtained for up to four layers of graphene in comparison to ITO. Our findings suggest that replacing ITO with monolayer graphene in organic solar cells yields comparable performance. Due to the increased optical absorption, organic solar cells with four-layer graphene (with the same sheet resistance as ITO at 30$\Omega/\Box$) are capable of attaining at least 92% of the same OPV device with an optimized ITO electrode for both normal and angular AM1.5G illumination.**

***Index Terms*—Computational modeling, Organic semiconductors, Photovoltaic cells, Thin film devices.**

I. Introduction

GRAPHENE, an isolated graphite plane, is actually crystallized carbon in a two dimensional form [1]. Since its extraction from graphite compounds, its electronic and optical properties have been extensively studied [2]. It was found to exhibit high optical transparency [3], electrical conductivity [4], as well as chemical and thermal stabilities amongst others. These excellent properties make graphene an ideal candidate for the replacement of a commonly used transparent conducting oxide, Indium Tin Oxide (ITO), prevalently used in the electronic displays and solar cell industries [5], [6]. Moreover, graphene is much more flexible than the brittle ITO, thus graphene is also viewed as an enabler in flexible electronics, in particular organic solar cells.

Although graphene has been shown to exhibit excellent optical transmittance of $> 90\%$, organic photovoltaic (OPV) devices which use graphene as the transparent electrode have not yielded better performance as compared to ITO based devices. For instance, Wu *et. al.* used solution-processed functionalized graphene films of 4–7 nm as transparent electrodes in a bilayer CuPc/C_{60} organic solar cell, and demonstrated power conversion efficiency (PCE) less than 50% of the reference cell PCE which uses ITO [7]. Similarly, Wang *et. al.* have demonstrated that using non-covalent modification of graphene transparent electrode, the PCE of a typical conjugated polymer poly(3-hexyl)thiophene:phenyl-C_{61}-butyric acid methyl ester or P3HT:PCBM bulk-heterojunction photovoltaic device with graphene transparent anode is about 55% of the ITO based device PCE of 3.1% [8]. A recent improvement of the same P3HT:PCBM device by the same group with four-layer graphene electrode attained 83.3% of the PCE of the same device with ITO [9]. For small molecule OPV devices, chemical vapor deposited graphene electrode has brought the PCE of multilayer graphene based CuPc:C_{60} OPV device, which is 1.18%, to nearly 93% of the 1.27% PCE of the ITO based OPV device [10]. Besides chemical vapor deposition, attempts to p-dope graphene with $AuCl_3$ in nitromethane have been shown to produce graphene with much smaller sheet resistance. Their PCE of a three-layer graphene based CuPc:C_{60} OPV device is 1.63% as compared to 1.77% PCE of the similar ITO device [11].

In this manuscript, we evaluate the potential of doped graphene as an alternative to the typical transparent electrode made of ITO in terms of its transmittance and optical absorption. Some of the questions which we will attempt to answer include: (1) Is it possible to improve the performance of organic solar cells by replacing ITO with graphene? (2) Is the improvement or reduction in performance valid for different OPV systems with active layers that absorb in different range of optical wavelengths? (3) Can we improve the angular absorption of the active layers by replacing ITO with graphene?

II. Graphene/ITO on Glass

To determine the impact of replacing ITO with graphene, we first look at a simple Glass(1.1mm)/ITO/Air or Glass(1.1mm)/Graphene/Air configuration (inset of Fig. 1). Normally incident monochromatic plane waves illuminate the bilayer structure (i.e light passes through glass first and then graphene or ITO as in a typical organic solar cell).

The integral transmittance $T_{\rm int}$ through the structure for λ = 350–800 nm is determined by weighting the transmission coefficient to account for the different intensities of the Air Mass 1.5 Global (AM1.5G) solar illumination (from $\lambda = 350 - 800$ nm) and normalized by the incident power of the spectrum given as

$$T_{\rm int} = \frac{\int_{\lambda=350nm}^{\lambda=800nm} T(\lambda)S(\lambda)d\lambda}{\int_{\lambda=350nm}^{\lambda=800nm} S(\lambda)d\lambda}, \qquad (1)$$

where $S(\lambda)$ is the AM1.5G solar spectrum, $T(\lambda) = \frac{P_{bottom}(\lambda)}{I_0}$ is the normalized wavelength-dependent transmittance of Glass(1.1 nm)/ITO or Graphene/Air configuration at each λ and is computed by solving the Maxwell's Equations using the transfer matrix method [12], $P_{bottom}(\lambda) = \vec{E} \times \vec{H}$ is the

All the authors except Choon How Gan are from the Electronics & Photonics Department of A*STAR Institute of High Performance Computing, Singapore.

Choon How Gan was previously the Electronics & Photonics Department of A*STAR Institute of High Performance Computing during the course of this work and he is currently with the College of Engineering, Mathematics and Physical Sciences, University of Exeter, Exeter EX4 4QF, United Kingdom.

Corresponding E-mail: kohws@ihpc.a-star.edu.sg

Poynting vector (i.e. $\vec{E}$ is the electric field vector and $\vec{H}$ is the magnetic field vector) taken below the graphene (ITO) layer, after the light passes through it. Here, I_0 taken as 1 W/cm^2 is the reference incident light intensity. In the computation of $T(\lambda)$, the relative permittivity of glass is assumed to be 2.2201 and the complex relative permittivity of ITO is taken from Ref. [13]. The frequency-dependent optical conductivity $\sigma(\omega)$ of graphene is computed taking the carrier mobility to be $\mu_m = 9000$ cm^2/Vs, which is typical of measured values [14], [15]. Here $\omega = 2\pi c/\lambda$ is the angular frequency with c being the speed of light in vacuum. Let us take the carrier density to be $n_c = 6 \times 10^{12}$ cm^{-2}, corresponding to a sheet resistance $\rho = 1/(n_c e \mu_m) \approx 120\Omega/\square$ for doped graphene produced by roll-to-roll technology [16]. We may proceed to estimate the chemical potential $\mu_c \approx \hbar v_F \sqrt{n_c \pi} \sim 0.3$ eV ($\mu_c \gg K_B\tau \sim 26$ meV, temperature τ taken to be 300 K), where $v_F \approx 10^8$ cm/s is the Fermi velocity. As the sheet resistance directly affects the performance of a solar cell, we have employed analytical calculations for $\sigma(\omega)$ so that one may quantify changes in the optical conductivity of graphene with respect to variations in the sheet resistance or carrier density. For small wavevectors $\mathbf{k}$ (i.e., $|\mathbf{k}|v_F \ll \omega$) and at high frequencies where $\omega \gg \tau_e^{-1}$ (τ_e being a phenomenological electron relaxation time in the order of 10^{-13}s) [17], the optical conductivity $\sigma(\omega) = \sigma^{\rm inter}(\omega) + \sigma^{\rm intra}(\omega)$ of graphene may be expressed as [18], [19]

$$\begin{aligned}\sigma^{\rm inter}(\omega) &= \frac{{\rm i}e^2\omega}{\pi\hbar^2}\int_0^\infty \frac{F(-\varepsilon)-F(\varepsilon)}{\omega^2-4(\varepsilon/\hbar)^2}\,d\varepsilon \\ &= \frac{e^2}{4\hbar}\left[1+\frac{\rm i}{\pi}\ln\frac{\hbar\omega-2\mu_c}{\hbar\omega+2\mu_c}\right], (\mu_c \gg K_B\tau) \quad (2)\end{aligned}$$

where $\sigma^{\rm inter}(\omega)$ takes into account interband electron transitions, and

$$\begin{aligned}\sigma^{\rm intra}(\omega) &= \frac{e^2}{{\rm i}\pi\hbar^2(\omega+{\rm i}\tau_e^{-1})}\int_0^\infty \varepsilon\left(\frac{\partial F(\varepsilon)}{\partial\varepsilon}-\frac{\partial F(-\varepsilon)}{\partial\varepsilon}\right)d\varepsilon \\ &= \frac{e^2\mu_c\tau_e(1+{\rm i}\omega\tau_e)}{\pi\hbar^2(1+\omega^2\tau_e^2)}, (\mu_c \gg K_B\tau), \quad (3)\end{aligned}$$

where $\sigma^{\rm intra}(\omega)$ takes into account intraband electron-photon scattering, and $F(\varepsilon) = (1+\exp[(\varepsilon-\mu_c)/K_B\tau])^{-1}$ is the Fermi-Dirac distribution. For the range of frequencies considered in Eq. 1, $\omega^2\tau_e^2 \gg 1$, $\Re(\sigma^{\rm intra}) \approx 0$ and

$$\sigma(\omega) \approx \frac{e^2}{4\hbar}\left[1+\frac{\rm i}{\pi}\left\{\ln\frac{\hbar\omega-2\mu_c}{\hbar\omega+2\mu_c}+\frac{4\mu_c}{\hbar\omega}\right\}\right]. \quad (4)$$

The conductivity for few-layer graphene may be estimated as $N\sigma(\omega)$, where N is the number of layers ($N < 10$) [20]. In calculating the transmission coefficient $T(\lambda)$, it is taken that monolayer graphene has an effective thickness $t_g \sim 0.5$ nm and an equivalent dielectric constant $\epsilon_g(\omega) = 1 + {\rm i}\sigma(\omega)/(\omega\epsilon_0 t_g)$ [17], [21].

Figure 1 shows that monolayer graphene has a transmittance $T(\lambda) > 90\%$ over the 350–800 nm wavelength range, which results in better integral transmittance $T_{\rm int}$ than 130 nm thick ITO with $T_{\rm int} = 87.1\%$. However, as the number of graphene layers increases, the integral transmittance decreases by 1.68% to 1.48% for each additional layer of graphene. Note that with graphene on glass, the reduction of the the transmittance (after scaling with the AM1.5G solar spectrum) is no longer a function of the fine structure constant where we would expect a reduction of the transmittance by 2.3% [3], [22] for each additional layer of graphene. This decoupling of the reduction in the transmittance from the expected 2.3% reduction per additional graphene layer can be attributed primarily to (1) the weighting of the wavelength-dependent transmittance $T(\lambda)$ based on the AM1.5G solar spectrum, and (2) to a lesser extent the presence of the Glass substrate. For transmittance $T_{\rm int} > 85\%$, the thickness of ITO has to be either less than 20 nm or greater than 100 nm. In the commercial use of ITO, the typical thickness usually adopted is more than 100 nm to ensure that the electrical conductivity is not compromised [7], [10]. Therefore, Fig. 1 suggests that it is possible to achieve comparable or even higher transmittance than provided by ITO with four or less layers of graphene. In terms of the sheet resistance, $N = 4$ layers of graphene (sheet resistance ~30 Ω/□) is roughly equivalent to ITO on glass (sheet resistance ~20-30 Ω/□). The linear decrease in the transmittance gave an indication that absorption may be a significant factor for graphene as the number of layers is increased. On the other hand, with ITO as the transparent electrode, optical interference seems to have a much more important effect since it is mostly transparent in the wavelengths of interest for organic solar cells.

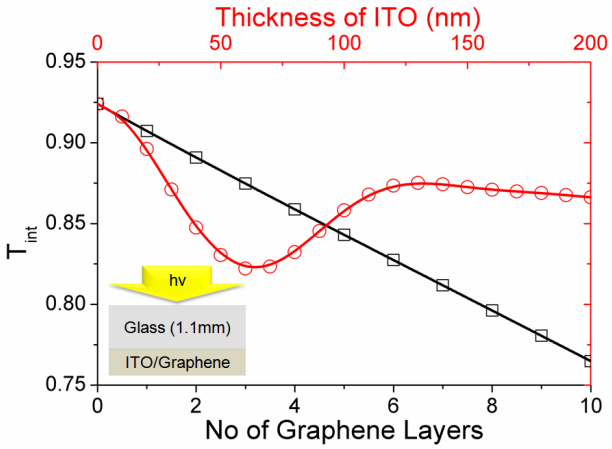

Fig. 1. (Color online) Integral transmittance $T_{\rm int}$ of light (λ = 350–800 nm) illuminating 1.1 mm thick glass and graphene (ITO) as a function of number of graphene layers (ITO thickness).

III. Graphene as a Transparent Electrode in P3HT:PCBM Organic Solar Cell

Next, we consider the use of graphene to replace ITO transparent electrode in a well studied conjugated polymer based organic bulk heterojunction solar cell with the following structure as shown in Fig. 2(a): Glass(1.1mm)/ ITO(130nm)/ PEDOT:PSS(45nm)/ P3HT:PCBM(75nm)/ Ca(10nm)/ Ag(100nm). The wavelength-dependent complex relative permittivities of the hole-transporting poly(3,4-ethylenedioxythiophene) poly(styrenesulfonate) (PEDOT:PSS)

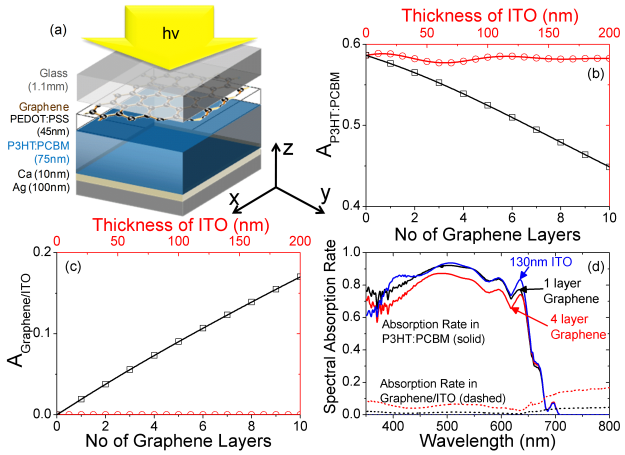

Fig. 2. (Color online) (a) Structure of P3HT:PCBM organic bulk heterojunction solar cell with graphene as the transparent electrode. Normalized absorbed power of light in (b) P3HT:PCBM active layer and (c) graphene and ITO, as a function of number of graphene layers (and ITO thickness) under AM1.5G solar illumination from $\lambda = 350 - 800$ nm. (d) Spectral absorption rate in P3HT:PCBM (solid lines), graphene and ITO (dashed lines) for the OPV device with monolayer graphene, four-layer graphene, and 130 nm thick ITO.

layer, poly(3-hexylthiophene):methanofullerene-phenyl C_{61}-butryic acid methyl ester (P3HT:PCBM in 1:0.8 weight ratio) active layer, calcium (Ca) electron transporting layer and silver (Ag) back reflector are taken from Ref. [13]. We have to emphasize that the choice of the dimensions and structure of the P3HT:PCBM OPV device is such that the actual optimized experimental device were shown to exhibit power conversion efficiencies of more than 3.5% as shown in Refs. [13], [23].

To quantify and compare the performance of the P3HT:PCBM OPV device, we have computed the normalized absorbed power in the active layer and also the transparent electrode (i.e. graphene and ITO). The normalized absorbed power of the layer of interest is given by

$$A = \frac{\int_{\lambda=350nm}^{\lambda=800nm} [P_{top}(\lambda) - P_{bottom}(\lambda)]\ S(\lambda)\ \ d\lambda}{\int_{\lambda=350nm}^{\lambda=800nm} S(\lambda)\ d\lambda} \qquad (5)$$

where $P_{top}(\lambda)$ and $P_{bottom}(\lambda)$ are the Poynting vectors of the top and bottom interface of the layer of interest.

Figure 2(b) illustrates the normalized absorbed power in the P3HT:PCBM active layer with respect to the integrated incident power of the AM1.5G solar spectrum, over $\lambda = 350 - 800$ nm, $S_{\text{int}} = 575.35$ W/m^2 at normal incidence. We observed that the normalized power absorbed by the P3HT:PCBM photoactive layer decreases with number of graphene layers (from 57.6% for the monolayer to 45.0% for ten-layer of graphene), while with up to 200nm thick ITO, it is about 58.9–57.8%. This shows that even with $> 90\%$ transmittance for monolayer graphene on glass, the performance of the P3HT:PCBM device is only comparable to that of an ITO based device, measured in terms of the power absorbed in P3HT:PCBM. With four-layer of graphene (i.e. sheet resistance $\sim 30\Omega/\Box$), the amount of optical power absorbed in P3HT:PCBM is 53.9% or 92.3% of the same OPV device with 130 nm thick ITO transparent electrode. The difference in the power absorbed in the P3HT:PCBM active layer with four-layer graphene or 130 nm thick ITO illustrates that while the graphene electrode allows comparable amount of light to enter the active layer, the amount of light absorbed by the P3HT:PCBM after accounting for multiple passes and optical interference is lesser compared to the case when ITO electrode is used.

The normalized absorbed power for both graphene and ITO in the organic solar cell configuration is plotted in Fig. 2(c). It is evident that the absorption in the thin graphene electrode ($\sim$1.93% for monolayer of graphene) is much higher than that of ITO (0.0006% for 130 nm thick ITO) even for a monolayer graphene. Therefore, it is obvious that the absorption in graphene is a limiting mechanism to replace ITO as a transparent electrode. Although, graphene absorption losses are so much higher than ITO, it is instructive to look at the normalized spectral absorption rate of P3HT:PCBM for both graphene and ITO electrodes. To understand why the normalized absorbed power in P3HT:PCBM is just slightly smaller by 4% between the monolayer graphene case and 130 nm thick ITO reference case even though the absorption of graphene is almost 10 times higher ($\sim$1.93% for monolayer graphene case and 0.0006% for 130 nm ITO reference case), we plot the normalized spectral absorption profile of P3HT:PCBM for both the graphene and ITO electrodes.

Figure 2(d) shows the normalized spectral absorption in P3HT:PCBM for monolayer graphene, four-layer graphene, and 130 nm ITO before weighting with the AM1.5G solar spectrum for λ = 350–800 nm. We observed that compared to ITO, graphene facilitates broadband absorption of light for the whole range of wavelengths where P3HT:PCBM absorbs. Moreover, it is interesting to note that the monolayer graphene electrode performs just as well as the 130 nm thick ITO electrode at optical wavelengths (λ = 450–600 nm) even though the absorption of the graphene electrode is higher. With the four-layer graphene electrode, the absorption losses is the main performance limiting factor even though it has similar transmittance with the ITO on glass electrode as shown in Fig. 1.

Besides normal incidence, we calculated the absorption for obliquely incident light on both the graphene and ITO electrode P3HT:PCBM OPV device. Figure 3 presents the normalized absorbed power of the P3HT:PCBM active layer (with respect to the absorption of in P3HT:PCBM with 130nm thick ITO transparent electrode) as a function of the angle of incidence for OPV devices with monolayer and four-layer graphene. It is interesting to note that the P3HT:PCBM OPV device with ITO electrode absorbs well for the angle range of 0–45 degrees, but the OPV device with monolayer graphene absorbs slightly better in the range of 50-65 degrees. Ignoring the relevance of the sheet resistance, the use of graphene as an electrode may be advantageous for illumination at large angles leading to a wider angle of absorption of light. However, taking sheet resistance into account and assuming the same sheet resistance of $\sim 30\Omega/\Box$ for both four-layer graphene and 130nm ITO, the absorption in the four-layer graphene reduces the absorption in the photoactive layer for all angles. For

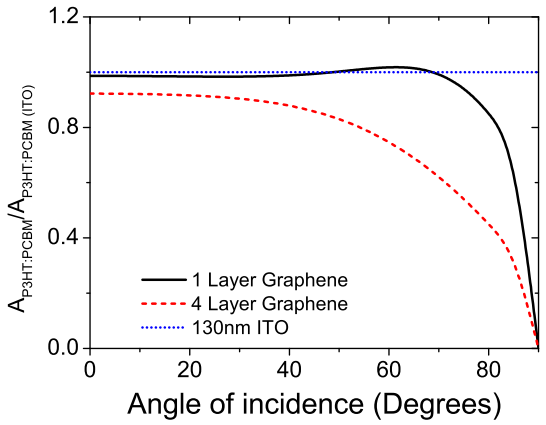

Fig. 3. (Color online) Normalized absorbed power of light in the P3HT:PCBM active layer for monolayer (black solid line) and four-layer graphene (red dashed line) transparent electrode with respect to the absorbed power in the same active layer with 160nm thick ITO electrode (blue dotted line) under AM1.5G solar illumination from $\lambda = 350 - 800$ nm at different angles of incident light.

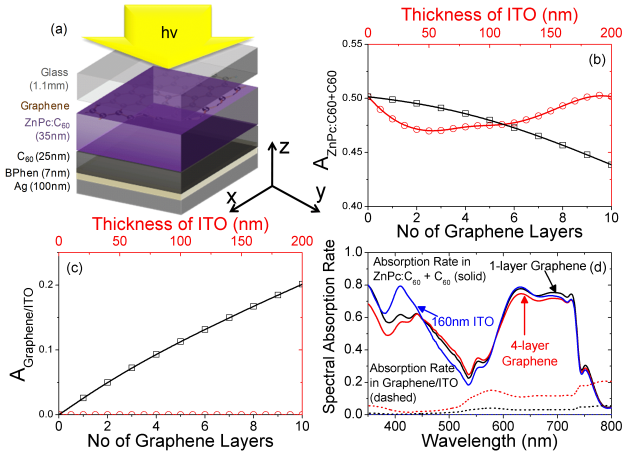

Fig. 4. (Color online) (a) Structure of ZnPc:C_{60} organic bulk heterojunction solar cell with graphene as the transparent electrode. Normalized absorbed power of light in (b) ZnPc:C_{60} and C_{60} active layer and (c) graphene and ITO, as a function of number of graphene layers (and ITO thickness) under AM1.5G solar illumination from $\lambda = 350 - 800$ nm. (d) Spectral absorption rate in ZnPc:C_{60} + C_{60} (solid lines), graphene and ITO (dashed lines) for the OPV device with monolayer, four-layer graphene and 160 nm thick ITO.

angles up to 30 degrees, four-layer graphene performs at about 90% as that of 130nm ITO electrode for the P3HT:PCBM OPV device, but for larger angles of AM1.5G illumination, the performance decreases quickly as the angle of illumination increases.

IV. Graphene as a Transparent Electrode in ZnPc:C_{60} Organic Solar Cell

Besides the P3HT:PCBM OPV device with an absorption spectrum between wavelengths λ =350-650nm, we also consider the use of graphene to replace ITO transparent electrode in a small molecule based organic bulk heterojunction solar cell which absorbs better in the near infrared wavelengths λ =450-750nm. The small molecule based organic solar cell structure is shown in Fig. 4(a): Glass(1.1mm)/ ITO(160nm)/ ZnPc(35nm)/ C_{60}(25nm)/ BPhen(7nm)/ Ag(100nm). The wavelength-dependent complex relative permittivities of the zinc phthalocyanine (ZnPc): fullerene (C_{60}) layer can be found in Ref. [24], while C_{60}, 4,7-diphenyl-1,10-phenanthroline (BPhen) exciton-blocking layer are characterized by ellipsometry and the corresponding permittivities are given in the appendix. Note that the structure and dimensions were reported working devices with 3.9% power conversion efficiency [25].

Figure 4(b) illustrates the normalized absorbed power in the ZnPc:C_{60} and C_{60} active layer with respect to the integrated incident power of the AM1.5G solar spectrum, over $\lambda = 350 - 800$ nm, $S_{\text{int}} = 575.35$ W/m^2. We observed that the normalized power absorbed by the photoactive layer decreases with number of graphene layers (from 49.9% for the monolayer to 44.0% for 10 layers of graphene), while with up to 200nm thick ITO, it is about 50.3–47%. With four-layer graphene, the amount of optical power absorbed in ZnPc:C_{60}+C_{60} is 48.6% (or 98.6% that of the same ZnPc:C_60 OPV device with 160 nm thick ITO transparent electrode). The small difference in the power absorbed in the ZnPc:C_{60}+C_{60} active layer between four-layer graphene and 160 nm thick ITO illustrates that the absorption in graphene has a less prominent effect on the absorption in the active layer when the photoactive layer is able to absorb more light in the near infrared wavelengths. The normalized absorbed power for both graphene and ITO in the organic solar cell configuration is plotted in Fig. 4(c). It is obvious that absorption in graphene is also the limiting factor for the ZnPc:C_{60} OPV device, which similar to the case for the P3HT:PCBM device discussed in Section III. Note that recent comparison of doped graphene with ITO in small molecule OPV devices similar to ZnPc:C_60 shows that doped graphene devices exhibit 92-93% of the PCE of ITO control devices, This is very close to the results which we have shown in this this section from purely an optical perspective and we would not expect multilayer doped graphene (or four-layer graphene as considered here) to be able to outperform ITO based devices if the sheet resistance has to be kept to a minimum of $\sim 30\Omega/\square$ assumed here.

Figure 4(d) shows the normalized spectral absorption in ZnPc:C_{60}+C_{60} for mono- and four-layer graphene and 160 nm ITO before weighting with the AM1.5G solar spectrum for λ = 350–800 nm. It is surprising to see that having ITO as the transparent electrode allows higher absorption than monolayer graphene electrode at two wavelength bands (i.e. λ = 400–450nm) for both P3HT:PCBM and ZnPc:C_{60} bulk-heterojunction devices. For λ = 450–570nm, optical interference due to the thick ITO electrode reduces the absorption of light in the active layer of the ZnPc:C_{60} device and even the same device with four-layer graphene exhibits higher light absorption ability in this range of wavelengths. It is also interesting to note that for $\lambda > 700$nm, the ZnPc:C_{60} OPV device with monolayer or four-layer of graphene allows better or comparable light absorption in the active layer than the same OPV device with 160nm thick ITO as the transparent electrode. Therefore, we can deduce that even without the advantage of optical interference, monolayer to four-layer of graphene is slightly more transparent to near infra-red light

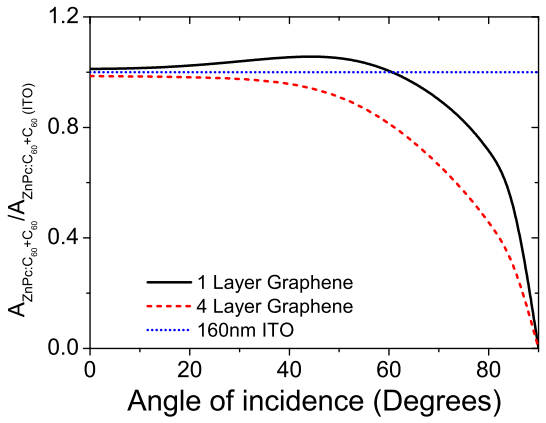

Fig. 5. (Color online) Normalized absorbed power of light in the ZnPc:C_{60} and C_{60} active layer for monolayer (black solid line) and four-layer graphene (red dashed line) transparent electrode with respect to the absorbed power in the same active layer with 160nm thick ITO electrode (blue dotted line) under AM1.5G solar illumination from $\lambda = 350 - 800$ nm at different angles of incident light.

and allows the NIR light to be absorbed more efficiently by the active layer in ZnPc:C_{60} OPV device.

The angular response of a graphene electrode based ZnPc:C_{60} is slightly different from that of the P3HT:PCBM solar cell. Figure 5 shows that monolayer graphene electrode enables more light to be absorbed by the ZnPc:C_{60} active layer for angle of incidence between 0-60 degress. Similar to the P3HT:PCBM case, if we take sheet resistance into account and select four-layer graphene as a transparent conductor, the absorption in the ZnPc:C_{60}+C_{60} active layer also decreases due to high absorption in the four-layer graphene transparent electrode for all angles of AM1.5G illumination. As compared to the P3JT:PCBM device, the performance of the ZnPc:C_{60} OPV device with four-layer graphene is maintained at 90% that of the same OPV device with 160nm ITO electrode for angles of illumination up to 40 degrees.

V. Discussion

In the previous sections, we have illustrated that the the main reason for reduced transmittance and lower optical absorption in doped graphene is mostly due to the absorption of the graphene material itself. On the other hand, precise tuning of the thickness of ITO is essential to optimize optical interference in the OPV device configuration. We must emphasize that the computed dielectric permittivity of doped graphene is based on the best experimentally determined sheet resistance for doped graphene by roll-to-roll processing. However, we note that the change of sheet resistance (due to different doping compounds on graphene) on the mobility of charge carriers for a monolayer graphene does not change the optical conductivity (and the corresponding dielectric permittivity) significantly. For instance, reducing the mobility from 9000 cm^2/Vs to 5000 cm^2/Vs only change the dielectric permittivity by less than 0.0001%. Therefore, we do not see a huge difference of our optical results even if graphene is doped with different chemical compounds to improve its sheet resistance to achieve charge mobilities of $>$ 5000 cm^2/Vs. However electrically, better sheet resistance (i.e. $\ll$ 120 $\Omega/\square$) for monolayer graphene, which implies a mobility $\gg$ 9000 cm^2/Vs will allow the reduction of four-layer graphene to three-layer graphene to maintain the minimum sheet resistance of 30 $\Omega/\square$ assumed here. But such a variation do not change our conclusion based on our optical results significantly.

Besides chemically doped graphene considered in this study, it has come to our attention that intercalating few-layer graphene (FLG) with ferric chloride ($FeCl_3$) has enabled rapid sheet resistance reduction of multilayer graphene from $>$ $1000\Omega/\square$ for 2-layer graphene to $8.8\Omega/\square$ for 5-layer graphene [26] with high optical transparency greater than 84%. Our findings here are expected to hold also for the intercalated FLG electrodes in Ref. [26] as the charge density and mobility values used for calculating the optical conductivity of graphene have the same order of magnitude.

Without considering the effect of sheet resistance on the carrier collecting efficiency of the OPV devices, we are presenting the best case where monolayer graphene works best optically. Therefore, the results for monolayer graphene OPV devices effectively presents the best case scenario (or the performance limit) in terms of the performance of graphene as a transparent electrode and compare it directly with the same OPV device with optimized ITO thickness. Therefore, the performance limits of monolayer graphene for conjugated polymer P3HT:PCBM and small molecule ZnPc:C_{60} OPV devices are 99% and 101% that of the same device with optimized ITO as the transparent electrode.

On the other hand, if we consider $\sim$ $30\Omega/\square$ as the maximum sheet resistance required for practical OPV devices, four-layer graphene which is able to offer comparable light transmittance as ITO is chosen. Our simulation results illustrate that optical absorption in the active layer drops from 99% and 101% (for the monolayer case) to about 92% and 98% (for the four-layer graphene case) to that an ITO electrode OPV devices for P3HT:PCBM and ZnPc:C_{60} OPV cells respectively. A comparison with the best performing (in terms of the PCE of an ITO based OPV device) OPV devices are 83.3% for the conjugated polymer P3HT:PCBM device [9] and 93% for small molecule CuPc:C_{60} (similar absorption spectrum as ZnPc:C_{60}) device [10] indicates that our optical simulation is able to predict the upper limit of the performance of multilayer graphene electrodes in real OPV devices. Thus, we would expect that there are still some room for improvement in the processing of graphene to improve the sheet resistance of the doped graphene synthesized to that of the roll-to-roll graphene sheets fabricated in Ref. [16].

In terms of angular response, the absorption in the active layers of both organic bulk heterojunction solar cell considered here are comparable for monolayer graphene and ITO but graphene seems to have a slight advantage for obliquely incident light around 45 degrees. Monolayer graphene performs better for obliquely incident light because graphene allows more light to pass through at all angles as it is very thin, whereas optical interference plays a more important part for ITO and the thickness of ITO is chosen such that the absorption in the active layer is maximized for normally incident

light only. With four-layer doped graphene as the transparent electrode, the angular performance for both P3HT:PCBM and ZnPc:C_{60} OPV devices with doped graphene electrode are poorer than using ITO as the transparent electrode, mainly due to increased absorption (i.e. decreased transmittance) through the four-layer graphene electrode. Thus, we should be mindful that having multiple layers of graphene, with low sheet resistance, as the transparent electrode in OPV devices also reduce the angular absorption of the solar irradiation as compared to ITO.

Last but not least, we observed from the spectral absorption plots in Figs. 3(d) and 5(d) for both P3HT:PCBM and ZnPc:C_{60} OPV devices and found that graphene performs better for the small molecule ZnPc:C_{60} device than for the conjugated polymer P3HT:PCBM when compared to their respective optimized ITO based device. This noted difference is because optical interference provided by ITO not only induce enhanced absorption in the active layer for certain wavelength range (i.e. 400-440nm and 640-660nm for P3HT:PCBM and 390-440nm for ZnPc:C_{60}), but also reduce absorption for other wavelength range (i.e. 350-380nm for P3HT:PCBM and 450-70nm for ZnPc:C_{60}) Graphene, on the other hand, allows rather uniform transmission over the whole optical spectrum and its own absorption is the only limiting factor. Therefore, P3HT:PCBM which have a narrow wavelength of absorption ($\sim$ 350-650nm) will benefit more from optical interference by ITO as compared to ZnPc:C_{60} OPV device which have a much wider range of absorption ($\sim$ 350-750nm). Thus, we would expect graphene to outperform ITO as a transparent conductor for organic solar cells with active materials that have a much broader absorption spectrum than ZnPc:C_{60} OPV device as it allow light of a broad range of wavelengths to reach the active layer more effectively as compared to limited enhancement (with some trade-offs) by optical interference with ITO.

VI. Summary

In summary, we have based our computation of the dielectric permittivity of graphene on experimentally determined sheet resistance for doped graphene by roll-to-roll processing (which is a promising technology for large scale production of substrate for organic solar cells). From a purely optical perspective, it has been shown that monolayer to four-layer doped graphene sheets has higher or comparable light transmittance than ITO. Considering the best case scenario, where the effect of sheet resistances are ignored, monolayer graphene as the transparent electrode gives the same performance as an optimized ITO electrode. For practical purposes, we have also considered four-layer graphene where the sheet resistance is similar to current ITO deposition technology at $\sim 30\Omega/\square$. Our findings predict that replacing ITO with four-layer doped graphene in both P3HT:PCBM and ZnPc:C_{60} organic solar cell yields slightly poorer (or 92% and 98%) optical performance as compared to the typical ITO transparent electrode. While it is not possible to have better performance by replacing ITO with four-layer graphene, we found that the optical absorption in the active layer for ZnPc:C_{60} OPV devices (with a doped graphene) is better than that of the P3HT:PCBM device

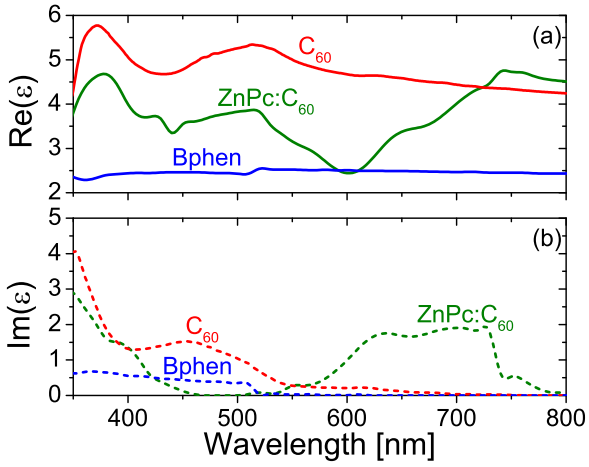

Fig. 6. (Color online) Real and imaginary part of the relative dielectric permittivity (ϵ)of Zinc phthalocyanine (ZnPc), Carbon-60 fullerene (C_{60}) and 4,7-diphenyl-1,10-phenanthroline (Bphen) for wavelengths 350-800nm.

(with the same doped graphene electrode) when compared to their counterpart with ITO electrode. In addition, we note that monolayer graphene electrode has comparable angular response as ITO, and the more practical four-layer graphene electrode can still performs at a maximum of 98% of the typical ITO electrode for all angles of solar illumination. Thus, from an optical perspective, graphene is indeed a viable alternative to ITO (i.e. four-layer graphene with sheet resistance of $\sim 30\Omega/\square$ have more than 90% the performance of optimized ITO electrode) for both P3HT:PCBM and ZnPc:C_{60} OPV devices considered here.

Acknowledgment

The author would like to thank Dr Wang Xizu, Goh Wei Peng and team from Institute of Materials Research and Engineering for sharing their measured data on the optical properties of the ZnPc:C_{60} bulk heterojunction photovoltaic device. We would also like to acknowledge Dr Li Erping for his valuable comments on the manuscript.

Appendix

The dielectric permittivities of all the materials (except graphene) used in this manuscript is measured using variable angle spectroscopic ellipsometry. The real and imaginary parts of the relative dielectric permittivity of ZnPc:C_{60}, C_{60}, Bphen, are shown in Fig. 6(a) and (b) respectively.

References

[1] Q. Liu, Z. F. Liu, X. Y. Zhang, L. Y. Yang, S. G. Yin, and Y. S. Chen. "Organic photovoltaic cells based on an acceptor of soluble graphene," *Appl. Phys. Lett.* vol. 92, no. 22, pp. 223303, Jun 2008.

[2] F. Bonaccorso, Z. Sun, T. Hasan, and A. C. Ferrari. "Graphene photonics and optoelectronics," *Nat. Photonics* vol. 4, pp. 611-622, Sep 2010.

[3] R. R. Nair, P. Blake, A. N. Grigorenko, K. S. Novoselov, T. J. Booth, T. Stauber, N. M. R. Peres, and A. K. Geim. "Fine Structure Constant Defines Visual Transparency of Graphene,"" *Science* vol. 320, no. 5881, pp. 1308, Jun 2008.

[4] A. K. Geim and K. S. Novoselov. "The rise of graphene," *Nat. Mat.* vol. 6, pp. 183-191, Mar 2007.

[5] A. M. Cox, A. Gorodetsky, B. Kim, K. S. Kim, Z. Jia, P. Kim, C. Nuckolls, and I. Kymissis. "Single-layer graphene cathodes for organic photovoltaics," *Appl. Phys. Lett.* vol. 98, no. 12, pp. 123303, Mar 2011.
[6] G. Jo, M. Choe, S. Lee, W. Park, T. H. Kahng, and T. Lee. "The application of graphene as electrodes in electrical and optical devices," *Nanotechnology* vol. 23, no. 11, pp. 112001, Jan 2012.
[7] J. Wu, H. A. Becerril, Z. Bao, Z. Liu, Y. Chen, and P. Peumans, Appl. Phys. Lett. "Organic solar cells with solution-processed graphene transparent electrodes," vol. 92, no. 26, pp. 263302, Jul 2008.
[8] Y. Wang, X. Chen, Y. Zhong, F. Zhu, and K. P. Loh. "Large area, continuous, few-layered graphene as anodes in organic photovoltaic devices," *Appl. Phys. Lett.* vol. 95, no. 6, pp. 063302, Aug 2009.
[9] Y. Wang, S. W. Tong, X. F. Xu, B. Ø" zyilmaz and K. P. Loh. "Interface Engineering of Layer-by-Layer Stacked Graphene Anodes for High-Performance Organic Solar Cells," *Adv. Mat.* vol. 23, no. 13, pp. 1514-1518, Mar 2011.
[10] L. G. De Arco, Y. Zhang, C. W. Schlenker, K. Ryu, M. E. Thompson, and C. Zhou. "Continuous, Highly Flexible, and Transparent Graphene Films by Chemical Vapor Deposition for Organic Photovoltaics," *ACS Nano* vol. 4, no. 5, pp. 2865-2873, Apr 2010.
[11] H. Park, J. A. Rowehl, K. K. Kim, V. Bulovic, and J. Kong. "Doped graphene electrodes for organic solar cells," *Nanotechnology* vol. 21, no. 50, pp. 505204, Nov 2010.
[12] B. S. Guru and H. R. Hiziroglu. *Electromagnetic Field Theory Fundamentals*. Cambridge University Press, UK , 2009, pp. 380-386.
[13] W. S. Koh, M. Pant, Yu. A. Akimov, W. P. Goh, and Y. Li. "Three-Dimensional Optoelectronic Model for Organic Bulk Heterojunction Solar Cells," *IEEE J. Photovoltaics* vol. 1, no. 1, pp. 84-92, Jul 2011.
[14] K. S. Novoselov, A. K. Geim, S. V. Morozov, D. Jiang, Y. Zhang, S.V. Dubonos, I. V. Grigorieva and A. A. Firsov. "Electric Field Effect in Atomically Thin Carbon Films ," *Science* vol. 306, no. 5696, pp. 666-669, Oct 2004.
[15] F. Schedin, A. K. Geim, S. V. Morozov, E. W. Will, P. Blake, M. I. Katsnelson and K. S. Novoselov. "Detection of individual gas molecules adsorbed on graphene," *Nat. Mat.* vol. 6, no. 9, pp. 652-655, Jul 2007.
[16] S. Bae, H. Kim, Y. Lee, X. Xu, J.-S. Park, Y. Zheng, J. Balakrishnan, T. Lei, H. R. Kim, Y. I. Song, Y.-J. Kim, K. S. Kim, B. Ozyilmaz, J.-H. Ahn, B. H. Hong, and S. Iijima. "Roll-to-roll production of 30-inch graphene films for transparent electrodes," *Nat. Nano.* vol. 5, no. 8, pp. 574-578, Aug 2010.
[17] Frank H. L. Koppens, Darrick E. Chang and F. Javier Garcia de Abajo. "Graphene Plasmonics: A Platform for Strong Light-Matter Interactions," *Nano Lett.* vol. 11, no. 8, pp. 3370-3377, Jul 2011.
[18] L. A. Falkovsky, and A. A. Varlamov. "Space-time dispersion of graphene conductivity," *Eur. Phys. J. B* vol. 56, no. 4, pp. 281-284, Apr 2007.
[19] C. H. Gan, H. S. Chu and E. P. Li. "Synthesis of highly confined surface plasmon modes with doped graphene sheets in the midinfrared and terahertz frequencies," *Phys. Rev. B* vol. 85, no. 12, pp. 125431, Mar 2012.
[20] Z. Ni, Y. Wang, T. Yu, and Z. Shen. "Raman Spectroscopy and Imaging of Graphene," *Nano Res.* vol. 1, no. 4, pp. 273-291, Oct 2008.
[21] C. H. Gan. "Analysis of surface plasmon excitation at terahertz frequencies with highly doped graphene sheets via attenuated total reflection," *Appl. Phys. Lett.* vol. 101, no. 11, pp. 111609 Sep 2012.
[22] L. Wu, H. S. Chu, W. S. Koh, and E. P. Li. "Highly sensitive graphene biosensors based on surface plasmon resonance," *Opt. Exp.* vol. 18, no. 14, pp. 14395-14400, Jun 2010.
[23] E. D. Palik, *Handbook of Optical Constants of Solids*. Academic, New York, 1998, pp. 355-356.
[24] X. Z. Wang, G. M. Ng, J. W. Ho, H. L. Tam and F. Zhu. "Efficient Semitransparent Bulk-Heterojunction Organic Photovoltaic Cells With High-Performance Low Processing Temperature IndiumTin Oxide Top Electrode," *IEEE J. Sel. Top. Quantum Electron.* vol. 16,no. 6, pp. 1685-1689, Dec 2010.
[25] W. Zeng, K. S. Yong, Z. M. Kam, F. Zhu and Y. Li. "Effect of blend layer morphology on performance of ZnPc:C60-based photovoltaic cells," *Appl. Phys. Lett.* vol. 97, no. 13, pp. 133304, Sep 2010.
[26] I. Khrapach, F. Withers, T. H. Bointon, F. Zhu and Y. Li. "Novel Highly Conductive and Transparent Graphene-Based Conductors," *Adv. Mat.* vol. 24, no. 21, pp. 2844-2849, Jun 2012.

Wee Shing Koh (S'03-M'07) was born in Singapore in 1977. He received his B.Eng.(Hons) and Ph.D. degrees in electrical and electronics engineering (EEE) from the Nanyang Technology University (NTU), Singapore, in 2002 and 2007, respectively.

He joined the A*STAR Institute of High Performance of High Performance Computing (IHPC), Singapore, as a Research Engineer and has been with IHPC since Jun 2006. He is recently awarded the inaugural IHPC Independent Investigatorship in late 2010 and is currently an IHPC Independent Investigator and Scientist at the Electronics & Photonics Department in IHPC. His research interests include organic solar cell device physics & simulation, computational plasmonics for thin film solar cells, sensors and various microelectronics applications. He is also interested in field emission theory, multi-dimensional space-charge-limited transport and particle-in-cell simulations for both micro- and nano-electronic applications.

He has published more than 35 journal and conference papers.

Choon How Gan Choon How Gan received his BEng degree in Electrical and Electronic Engineering from the Nanyang Technological University, Singapore, in 2001. Between 2002 and 2004, he was with the Defense Science Technology Agency as an engineer to provide technical consultation on underwater communication systems. He went to the University of North Carolina at Charlotte where he obtained the Optics Ph. D. degree in 2009. Upon graduation, he moved to France to join the Laboratoire Charles Fabry de l' Institut d'Optique for a two-year postdoctoral position. After that, he was research scientist with the Institute of High Performance Computing of A*STAR (Singapore) from 2011 to 2012. He is currently a postdoctoral fellow at the University of Exeter. His research interest includes plasmonic beam steering, single plasmon sources, optical coherence theory, and optical data storage.

Wee Kee Phua Wee Kee Phua is a research engineer at Institute of High Performance Computing Singapore. His current work focuses on plasmonics. He has a B.S. in Electrical and Electronics Engineering from the Nanyang Technological University, Singapore. He is currently pursuing a Ph.D. degree in Electrical and Computer Engineering from the National University of Singapore, Singapore.

Yuriy A. Akimov was born in Lugansk, Ukraine, in 1979. He received his M.Sc.(Hons) and Ph.D. degrees in plasma physics from V.N. Karazin Kharkiv National University, Ukraine, in 2002 and 2005, respectively.

From 2005 to 2008, he was with the Physics and Technology Department of V.N. Karazin Kharkiv National University, Ukraine. Since 2008, he is a Scientist at the Electronics and Photonics Department in the A*STAR Institute of High Performance Computing, Singapore. His research interests include nonlinear wave optics, plasma physics, nano-photonics and plasmonics.

Ping Bai Ping Bai (M99) received the B.Sc. degree from the University of Electronic Science and Technology of China in 1985, the M.Sc. degree from the Chinese Academy of Engineering Physics, Beijing, China, in 1988, and the Ph.D. degree from the Chinese Academy of Sciences, Beijing, China, in 1997, all in telecommunication and electronic systems.

From 1988 to 1994, he was an Engineer with the Chinese Academy of Engineering Physics. In 1997, he moved to Singapore and was a Chief Electronic Engineer with Transtech Electronics Pte Ltd. Since 1999, he has been with the Institute of High Performance Computing, A-Star, Singapore, where he is currently a Senior Scientist and Capability Group Manager with Plasmonics & Nanointegration Group. His research has focused on nanoelectronic and optoelectronic devices modeling and the electrical circuit and system design. Currently, he is actively involved in plasmonic and nanophotonic structures that are used for on-chip photonic-electronic integration and plasmonic sensing. He has authored or coauthored over 60 technical papers in international referred journals and conferences, and filed 6 technical disclosures and patents.